International Journal of Mathematical Archive-3(8), 2012, 2932-2945
Available online through www.ijma.info ISSN 2229 – 5046

EFFECTS OF THERMAL DIFFUSION AND DIFFUSION THERMO ON AN UNSTEADY MHD MIXED CONVECTION FLOW PAST AN ACCELERATED INFINITE VERTICAL PLATE WITH VISCOUS DISSIPATION

K. Sudhakar, R. Srinivasa Raju* and M. Rangamma

Department of Mathematics, University College of Science, Osmania University, Hyderabad, 500007, Andhra Pradesh, India

**Department of Mathematics, Padmasri Dr. B. V. Raju Institute of Technology, Narsapur, Medak, 502313, Andhra Pradesh, India*

(Received on: 19-07-12; Accepted on: 13-08-12)

ABSTRACT

The study of effects of thermal diffusion and diffusion thermo on an unsteady hydromagnetic mixed convective flow of incompressible and electrically conducting fluids past an accelerated infinite vertical porous plate in the presence of viscous dissipation has been made. Numerical solutions have been derived for the velocity, temperature and concentration fields, skin – friction, rate of heat and mass transfer by using Galerkin finite element method. The numerical results for some special cases were compared with Ramana Reddy et al. [16] and were found to be in good agreement. A parametric study illustrating the influence of different flow parameters on velocity, temperature and concentration fields are investigated. The skin – frictions at the plate due to velocity field and rate of heat and mass transfer due to temperature and concentration respectively are obtained in non – dimensional form. The effects of the different physical flow parameters on these respective flow fields are discussed through graphs and results are physically interpreted.

Key Words: *Thermal diffusion, Diffusion thermo, unsteady, MHD, Mixed convection flow, viscous dissipation, Galerkin finite element method.*

NOMENCLATURE

B_o	Magnetic field component along $y'-$ axis
c_p	Specific heat at constant pressure
Gr	Grashof number
Gc	Modified Grashof number
g	Acceleration of gravity
k'	The permeability of medium
K	The permeability parameter
M	Hartmann number
Pr	Prandtl number
Sc	Schmidt number
Sr	Thermal diffusion (Soret number)
Du	Diffusion thermo (Dufour number)
Ec	Eckert number
D	Chemical molecular diffusivity
T'	Temperature of fluid near the plate
T'_w	Temperature of the fluid far away of the fluid from the plate
T'_∞	Temperature of the fluid at infinity
T_m	Mean fluid temperature
C	Concentration of the fluid
C'	Concentration of fluid near the plate
D_m	Mass diffusivity
k_T	Thermal diffusion ratio
c_s	Concentration susceptibility
C'_w	Concentration of the fluid far away of the fluid from the plate
C'_∞	Concentration of the fluid at infinity
t'	Time in x', y' coordinate system
t	Time in dimensionless co – ordinates
u'	Velocity component in $x'-$ direction
u	Dimensionless velocity component in $x'-$ direction
v'	Velocity component in $y'-$ direction
v'_o	Dimensionless velocity component in $y'-$ direction
x', y'	Co – ordinate system
x, y	Dimensionless coordinates
U_o	Reference velocity

Greek symbols:

β	Coefficient of volume expansion for heat transfer
β^*	Coefficient of volume expansion for mass transfer
κ	Thermal conductivity of the fluid
σ	Electrical conductivity of the fluid
ν	Kinematic viscosity
θ	Non – dimensional temperature
ρ	Density of the fluid
ω	Angular frequency

1. INTRODUCTION

The problems of mixed convective MHD flows are of prime importance in a number of industrial applications in Geo – physical and Astro – Physical situations. The problem of convective MHD flows has wide range of publications in emerging fields viz granular insulation, geothermal systems in heating and cooling chambers, fossil fuel, combustion, energy process, solar energy and space vehicle re entry. Some examples in living organisms are fluid transport mechanism among which the blood flow in circulatory system, with flow in airways. A classical example is in nuclear power station where the separation of uranium U_{235} from U_{238} by gases diffusion takes place. When heat and mass transfer occur simultaneously between the fluxes, the driving potentials are of more intricate nature. An energy flux can be generated not only by temperature gradients but also by composition gradients as well. The energy flux caused by a composition gradient is called Dufour or diffusion thermo effect. Temperature gradients can also create mass fluxes, and this is the Soret or thermal diffusion effect. Generally, the thermal diffusion and the diffusion thermo effects are of smaller order magnitude than the effects prescribed by Fourier's or Fick's laws and are often neglected in heat and mass transfer processes. However, there are exceptions. The thermal diffusion effect, for instance, has been utilized for isotope separation and in mixture between gases with very light molecular weight (Hydrogen – Helium) and of medium molecular weight (Nitrogen – Air) the diffusion thermo effect was found to be of a magnitude such that it cannot be neglected (see Kafoussias *et al.* [8] and references therein).

In recent years, progress has been considerably made in the study of heat and mass transfer in magnetohydrodynamic flows due to its application in many devices. Abreu *et al*. [1] examined the boundary layer solutions for the cases of forced, natural and mixed convection under a continuous set of similarity type variables determined by a combination of pertinent variables measuring the relative importance of buoyancy force term in the momentum equation. Afify [2] carried out an analysis to study free convective heat and mass transfer of an incompressible, electrically conducting fluid over a stretching sheet in the presence of suction and injection with thermal diffusion and diffusion thermo effects. Alam *et al*. [3] studied numerically the Dufour and Soret effects on combined free-forced convection and mass transfer flow past a semi – infinite vertical plate under the influence of transversely applied magnetic field. Ambethkar [4] investigated numerical solutions of heat and mass transfer effects of an unsteady MHD free convective flow past an infinite vertical plate with constant suction.

Chin *et al*. [5] obtained numerical results for the steady mixed convection boundary layer flow over a vertical impermeable surface embedded in a porous medium when the viscosity of the fluid varies inversely as a linear function of the temperature. Gaikwad *et al*. [6] investigated the onset of double diffusive convection in two component couple of stress fluid layer with Soret and Dufour effects using both linear and non-linear stability analysis. Hayat *et al*. [7] discussed the effects of Soret and Dufour on heat and mass transfer on mixed convection boundary layer flow over a stretching vertical surface in a porous medium filled with a viscoelastic fluid. Kafoussias *et al*. [8] considered the boundary layer – flows in the presence of Soret, and Dufour effects associated with the thermal diffusion and diffusion thermo for the mixed forced natural convection. Lyubinova *et al*. [9] deals with the numerical investigation of the influence of static and vibrational acceleration on the measurement of diffusion and Soret coefficients in binary mixtures, in low gravity conditions. Mansour *et al*. [10] investigated the effects of chemical reaction, thermal stratification, Soret and Dufour numbers on MHD free convective heat and mass transfer of a viscous, incompressible and electrically conducting fluid over a vertical stretching surface embedded in a saturated porous medium.

Ming – chun *et al*. [11] studied Soret and Dufour effects in strongly endothermic chemical reaction system of porous media. Motsa [12] investigated the effects of Soret and Dufour numbers on the onset of double diffusive convection. Mukhopadhyay [13] performed an analysis to investigate the effects of thermal radiation on an unsteady mixed convection flow and heat transfer over a porous stretching surface in porous medium. Osalusi *et al*. [14] investigated thermo diffusion and diffusion thermo effects on combined heat and mass transfer of a steady hydromagnetic convective and slip flow due to a rotating disk in the presence of viscous dissipation and ohmic heating. Pal *et al*. [15] analyzed the combined effects of mixed convection with thermal radiation and chemical reaction on MHD flow of viscous and electrically conducting fluid past a vertical permeable surface embedded in a porous medium. Ramana Reddy *et al*. [16] discussed the effect of heat and mass transfer on mixed convective MHD flow past an accelerated infinite vertical porous plate. Shateyi [17] investigated thermal radiation and buoyancy effects on heat and mass transfer over a semi – infinite stretching surface with suction and blowing. Srihari *et al*. [18] discussed Soret effect on

unsteady MHD free convective mass transfer flow past an infinite vertical porous plate with oscillatory suction velocity and heat sink. More recently, Vempati *et al*. [19] studied numerically the effects of Dufour and Soret numbers on an unsteady MHD flow past an infinite vertical porous plate with thermal radiation.

Motivated by the above reference work and the numerous possible industrial applications of the problem (like in isotope separation), it is of paramount interest in this study to investigate the effects Soret and Dufour on MHD flow along a porous flat plate. Hence, the purpose of this paper is to extend the results of Ramana Reddy *et al.* [16] to study the more general problem which includes the Soret and Dufour effects on an unsteady MHD flow and heat transfer along a porous flat plate with mass transfer in presence of viscous dissipation. In this study, the effects of different flow parameters encountered in the equations are also studied. The problem is solved numerically using the Galerkin finite element method, which is more economical from the computational view point.

2. MATHEMATICAL ANALYSIS

Consider the unsteady mixed convection mass transfer flow of a viscous incompressible electrically conducting fluid past an accelerating vertical infinite porous flat plate in the presence of transversal magnetic field B_o. The x' – axis is directed upward along the plate and y' – axis normal to the plate with u, being the velocity component along the x' – axis. It is assumed that the plate is accelerating with a velocity $u = U_o$ in its own plane for $t' \geq 0$. The magnetohydro dynamic unsteady mixed convective boundary layer equations under the Boussinesq approximations are:

Continuity Equation:

$$\frac{\partial v'}{\partial y'} = 0 \Rightarrow v' = -v'_o \text{ (Constant)} \tag{1}$$

Momentum Equation:

$$\frac{\partial u'}{\partial t'} + v'\frac{\partial u'}{\partial y'} = g\beta\left(T' - T'_\infty\right) - \nu\frac{u'}{k'} + g\beta^*\left(C' - C'_\infty\right) + \nu\frac{\partial^2 u'}{\partial y'^2} - \frac{\sigma B_o^2}{\rho}u' \tag{2}$$

Energy Equation:

$$\frac{\partial T'}{\partial t'} + v'\frac{\partial T'}{\partial y'} = \frac{\kappa}{\rho\, c_p}\frac{\partial^2 T'}{\partial y'^2} + \frac{\nu}{c_p}\left(\frac{\partial u'}{\partial y'}\right)^2 + \frac{D_m k_T}{c_S c_P}\frac{\partial^2 C'}{\partial y'^2} \tag{3}$$

Concentration Equation:

$$\frac{\partial C'}{\partial t'} + v'\frac{\partial C'}{\partial y'} = D\frac{\partial^2 C'}{\partial y'^2} + \frac{D_m k_T}{T_m}\frac{\partial^2 T'}{\partial y'^2} \tag{4}$$

The boundary conditions of the problem are:

$$\left.\begin{aligned} t' \leq 0 &: \{\, u' = 0,\ v' = 0,\ T' = 0,\ C' = 0 \ \text{ for all } y' \\ t' \geq 0 &: \begin{cases} u' = U_O,\ v' = -v'_o,\ T' = T'_w,\ C' = C'_w \ \text{ at } y' = 0 \\ u' \to 0,\ T' \to T'_\infty,\ C' \to C'_\infty \ \text{ as } y' \to \infty \end{cases} \end{aligned}\right\} \tag{5}$$

Introducing the following non – dimensional variables and parameters,

$$\left.\begin{aligned} &y = \frac{y' v'_o}{\nu},\ t = \frac{t' v_o'^2}{4\nu},\ \omega = \frac{4\nu\omega'}{v_o'^2},\ u = \frac{u'}{U_o},\ M = \left(\frac{\sigma B_o^2}{\rho}\right)\frac{\nu}{v_o'^2},\ K = \frac{k' v_o'^2}{\nu^2}, Sc = \frac{\nu}{D}, \\ &\theta = \frac{T' - T'_\infty}{T'_w - T'_\infty},\ C = \frac{C' - C'_\infty}{C'_w - C'_\infty},\ \Pr = \frac{\nu}{k},\ Gr = \frac{\nu g\beta\left(T'_w - T'_\infty\right)}{U_o v_o'^3},\ Gc = \frac{g\beta^*\nu\left(C'_w - C'_\infty\right)}{U_o v_o'^3}, \\ &Ec = \frac{v_o'^2}{c_p\left(T'_w - T'_\infty\right)},\ Du = \frac{D_m k_T\left(C'_w - C'_\infty\right)}{c_S c_P\left(T'_w - T'_\infty\right)},\ Sr = \frac{D_m k_T\left(T'_w - T'_\infty\right)}{\nu T_m\left(C'_w - C'_\infty\right)} \end{aligned}\right\} \tag{6}$$

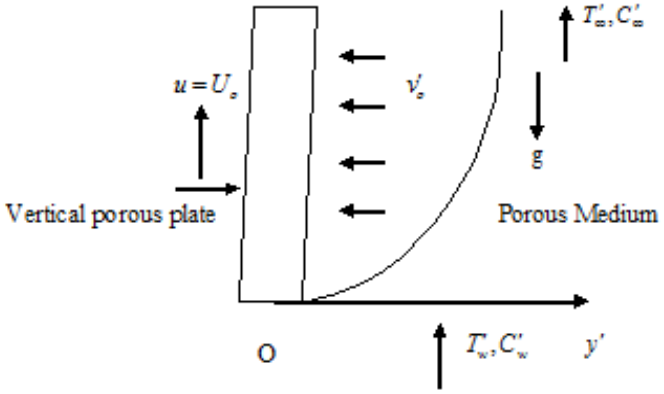

Figure 1. Physical sketch and geometry of the problem

Substituting (6) in equations (2), (3) and (4) under boundary conditions (5), we get:

$$\frac{\partial u}{\partial t} - \frac{\partial u}{\partial y} = (Gr)\theta + (Gc)C + \frac{\partial^2 u}{\partial y^2} - \left(M + \frac{1}{K}\right)u \tag{7}$$

$$\frac{\partial \theta}{\partial t} - \frac{\partial \theta}{\partial y} = \frac{1}{\Pr}\frac{\partial^2 \theta}{\partial y^2} + (Ec)\left(\frac{\partial u}{\partial y}\right)^2 + Du\left(\frac{\partial^2 C}{\partial y^2}\right) \tag{8}$$

$$\frac{\partial C}{\partial t} - \frac{\partial C}{\partial y} = \frac{1}{Sc}\frac{\partial^2 C}{\partial y^2} + Sr\left(\frac{\partial^2 \theta}{\partial y^2}\right) \tag{9}$$

The corresponding boundary conditions are:

$$\left.\begin{array}{l} u = 1,\ \theta = 1,\ C = 1 \ at\ y = 0 \\ u \to 0,\ \theta \to 0,\ C \to 0 \ as\ y \to \infty \end{array}\right\} \tag{10}$$

3. METHOD OF SOLUTION

By applying Galerkin finite element method for equation (7) over the element (e), $(y_j \le y \le y_k)$ is:

$$\int_{y_j}^{y_k} \left\{ N^T \left[\frac{\partial^2 u^{(e)}}{\partial y^2} - \frac{\partial u^{(e)}}{\partial t} + \frac{\partial u^{(e)}}{\partial y} - Au^{(e)} + P \right] \right\} dy = 0 \tag{11}$$

Where $P = (Gr)\theta_i^j + (Gc)C_i^j$, $A = M + \dfrac{1}{K}$;

Integrating the first term in equation (11) by parts one obtains

$$N^{(e)T}\left\{\frac{\partial u^{(e)}}{\partial y}\right\}_{y_j}^{y_k} - \int_{y_j}^{y_k}\left\{\frac{\partial N^{(e)T}}{\partial y}\frac{\partial u^{(e)}}{\partial y} + N^{(e)T}\left(\frac{\partial u^{(e)}}{\partial t} - \frac{\partial u^{(e)}}{\partial y} + Au^{(e)} - P\right)\right\} dy = 0 \tag{12}$$

Neglecting the first term in equation (12), one gets:

$$\int_{y_j}^{y_k}\left\{\frac{\partial N^{(e)T}}{\partial y}\frac{\partial u^{(e)}}{\partial y} + N^{(e)T}\left(\frac{\partial u^{(e)}}{\partial t} - \frac{\partial u^{(e)}}{\partial y} + Au^{(e)} - P\right)\right\} dy = 0$$

Let $u^{(e)} = N^{(e)}\phi^{(e)}$ be the linear piecewise approximation solution over the element (e),

$(y_j \le y \le y_k)$, where $N^{(e)} = \begin{bmatrix} N_j & N_k \end{bmatrix}$, $\phi^{(e)} = \begin{bmatrix} u_j & u_k \end{bmatrix}^T$ and $N_j = \dfrac{y_k - y}{y_k - y_j}, N_k = \dfrac{y - y_j}{y_k - y_j}$ are the basis functions. One obtains:

$$\int_{y_j}^{y_k} \left\{ \begin{bmatrix} N_j' N_j' & N_j' N_k' \\ N_j' N_k' & N_k' N_k' \end{bmatrix} \begin{bmatrix} u_j \\ u_k \end{bmatrix} \right\} dy + \int_{y_j}^{y_k} \left\{ \begin{bmatrix} N_j N_j & N_j N_k \\ N_j N_k & N_k N_k \end{bmatrix} \begin{bmatrix} \dot{u}_j \\ \dot{u}_k \end{bmatrix} \right\} dy - \int_{y_j}^{y_k} \left\{ \begin{bmatrix} N_j N_j' & N_j N_k' \\ N_j' N_k & N_k' N_k \end{bmatrix} \begin{bmatrix} u_j \\ u_k \end{bmatrix} \right\} dy$$

$$+ A \int_{y_j}^{y_k} \left\{ \begin{bmatrix} N_j N_j & N_j N_k \\ N_j N_k & N_k N_k \end{bmatrix} \begin{bmatrix} u_j \\ u_k \end{bmatrix} \right\} dy = P \int_{y_j}^{y_k} \begin{bmatrix} N_j \\ N_k \end{bmatrix} dy$$

Simplifying we get

$$\frac{1}{l^{(e)^2}} \begin{bmatrix} 1 & -1 \\ -1 & 1 \end{bmatrix} \begin{bmatrix} u_j \\ u_k \end{bmatrix} + \frac{1}{6} \begin{bmatrix} 2 & 1 \\ 1 & 2 \end{bmatrix} \begin{bmatrix} \dot{u}_j \\ \dot{u}_k \end{bmatrix} - \frac{1}{2l^{(e)}} \begin{bmatrix} -1 & 1 \\ -1 & 1 \end{bmatrix} \begin{bmatrix} u_j \\ u_k \end{bmatrix} + \frac{A}{6} \begin{bmatrix} 2 & 1 \\ 1 & 2 \end{bmatrix} \begin{bmatrix} u_j \\ u_k \end{bmatrix} = \frac{P}{2} \begin{bmatrix} 1 \\ 1 \end{bmatrix}$$

Where prime and dot denotes differentiation w.r.t y and time t respectively. Assembling the element equations for two consecutive elements $(y_{i-1} \le y \le y_i)$and $(y_i \le y \le y_{i+1})$ following is obtained:

$$\frac{1}{l^{(e)^2}} \begin{bmatrix} 1 & -1 & 0 \\ -1 & 2 & -1 \\ 0 & -1 & 1 \end{bmatrix} \begin{bmatrix} u_{i-1} \\ u_i \\ u_{i+1} \end{bmatrix} + \frac{1}{6} \begin{bmatrix} 2 & 1 & 0 \\ 1 & 4 & 1 \\ 0 & 1 & 2 \end{bmatrix} \begin{bmatrix} \dot{u}_{i-1} \\ \dot{u}_i \\ \dot{u}_{i+1} \end{bmatrix} - \frac{1}{2l^{(e)}} \begin{bmatrix} -1 & 1 & 0 \\ -1 & 0 & 1 \\ 0 & -1 & 1 \end{bmatrix} \begin{bmatrix} u_{i-1} \\ u_i \\ u_{i+1} \end{bmatrix} + \frac{A}{6} \begin{bmatrix} 2 & 1 & 0 \\ 1 & 4 & 1 \\ 0 & 1 & 2 \end{bmatrix} \begin{bmatrix} u_{i-1} \\ u_i \\ u_{i+1} \end{bmatrix} = \frac{P}{2} \begin{bmatrix} 1 \\ 2 \\ 1 \end{bmatrix} \tag{13}$$

Now put row corresponding to the node i to zero, from equation (13) the difference schemes with $l^{(e)} = h$ is:

$$\frac{1}{h^2}\left[-u_{i-1} + 2u_i - u_{i+1}\right] + \frac{1}{6}\left[\dot{u}_{i-1} + 4\dot{u}_i + \dot{u}_{i+1}\right] - \frac{1}{2h}\left[-u_{i-1} + u_{i+1}\right] + \frac{A}{6}\left[u_{i-1} + 4u_i + u_{i+1}\right] = P \tag{14}$$

Applying the trapezoidal rule, following system of equations in Crank – Nicholson method are obtained:

$$A_1 u_{i-1}^{n+1} + A_2 u_i^{n+1} + A_3 u_{i+1}^{n+1} = A_4 u_{i-1}^{n} + A_5 u_i^{n} + A_6 u_{i+1}^{n} + P^* \tag{15}$$

Now from equations (8) and (9) following equations are obtained:

$$B_1\theta_{i-1}^{n+1} + B_2\theta_i^{n+1} + B_3\theta_{i+1}^{n+1} = B_4\theta_{i-1}^{n} + B_5\theta_i^{n} + B_6\theta_{i+1}^{n} + Q^* \tag{16}$$

$$D_1 C_{i-1}^{n+1} + D_2 C_i^{n+1} + D_3 C_{i+1}^{n+1} = D_4 C_{i-1}^{n} + D_5 C_i^{n} + D_6 C_{i+1}^{n} + R^* \tag{17}$$

Where $A_1 = 2 + Ak + 3rh - 6r$, $A_2 = 8 + 4Ak + 12r$, $A_3 = 2 + Ak - 3rh - 6r$, $A_4 = 2 - Ak - 3rh + 6r$,
$A_5 = 8 - 4Ak - 12r$, $A_6 = 2 - Ak + 3rh + 6r$, $B_1 = 2(\mathrm{Pr}) + 3rh(\mathrm{Pr}) - 6r$, $B_2 = 8(\mathrm{Pr}) + 12r$,

$B_3 = 2(\mathrm{Pr}) - 3rh(\mathrm{Pr}) - 6r$, $B_4 = 2(\mathrm{Pr}) - 3rh(\mathrm{Pr}) + 6r$, $B_5 = 8(\mathrm{Pr}) - 12r$, $B_6 = 2(\mathrm{Pr}) + 3rh(\mathrm{Pr}) + 6r$,

$D_1 = 2(Sc) + 3rh(Sc) - 6r$, $D_2 = 8(Sc) + 12r$, $D_3 = 2(Sc) - 3rh(Sc) - 6r$, $D_4 = 2(Sc) - 3rh(Sc) + 6r$,

$D_5 = 8(Sc) - 12r$, $D_6 = 2(Sc) + 3rh(Sc) + 6r$, $P^* = 12Phk = 12hk(Gr)\theta_i^j + 12hk(Gm)C_i^j$,

$$R^* = 12kR = 12k(Sc)(Sr)\left(\frac{\partial^2 C_i^j}{\partial y^2}\right),$$

$$Q^* = 12kQ = 12k(\Pr)(Ec)\left(\frac{\partial u_i^j}{\partial y}\right)^2 + 12k(\Pr)(Du)\left(\frac{\partial^2 \theta_i^j}{\partial y^2}\right);$$

Here $r = \frac{k}{h^2}$ and h, k are mesh sizes along $y-$direction and time – direction respectively. Index i refers to space and j refers to the time. In the equations (15), (16) and (17) taking $i = 1(1)n$ and using boundary conditions (10), then the following system of equations are obtained:

$$A_i X_i = B_i;\ i = 1(1)3 \tag{19}$$

Where $A_i^{'}$s are matrices of order n and $X_i, B_i^{'}$s are column matrices having $n-$components. The solutions of above system of equations are obtained by using Thomas algorithm for velocity, temperature and concentration. Also, numerical solutions for these equations are obtained by $C-$programme. In order to prove the convergence and stability of Galerkin finite element method, the same $C-$programme was run with smaller values of h and k and no significant change was observed in the values of $u,\ \theta$ and C. Hence the Galerkin finite element method is stable and convergent.

4. SKIN – FRICTION AND RATE OF HEAT AND MASS TRANSFER

The skin – friction at the plate in the dimensionless form is given by $\tau = \left(\frac{\partial u}{\partial y}\right)_{y=0}$

The rate of heat transfer coefficient (Nu) at the plate is $Nu = \left(\frac{\partial \theta}{\partial y}\right)_{y=0}$

And the rate of mass transfer coefficient (Sh) at the plate is $Sh = \left(\frac{\partial C}{\partial y}\right)_{y=0}$

5. RESULTS AND DISCUSSIONS

The profiles of velocity, temperature and concentration are shown in the figures from (2) to (15) respectively. Figures (2) and (3) exhibit the effect of Grashof number and Modified Grashof numbers on the velocity profile with other parameters are fixed. The Grashof number (Gr) signifies the relative effect of the thermal buoyancy force to the viscous hydrodynamic force in the boundary layer. As expected, it is observed that there is a rise in the velocity due to the enhancement of thermal buoyancy force. Also, as Gr increases, the peak values of the velocity increases rapidly near the porous plate and then decays smoothly to the free stream velocity. The Modified Grashof number (Gc) defines the ratio of the species buoyancy force to the viscous hydrodynamic force. As expected, the fluid velocity increases and the peak value is more distinctive due to increase in the species buoyancy force. The velocity distribution attains a distinctive maximum value in the vicinity of the plate and then decreases properly to approach the free stream value. It is noticed that the velocity increases with increasing values of the Modified Grashof number (Gc). Figure (4) depicts the effect of Prandtl number on velocity profiles in presence of foreign species such as Mercury ($\Pr$ = 0.025), Air ($\Pr$ = 0.71), Water ($\Pr$ = 7.00) and Water at 4^oC ($\Pr$ = 11.62) are shown in figure (4). We observe that from figure (4) the velocity decreases with increasing of Prandtl number $(\Pr)$. The nature of velocity profiles in presence of foreign species such as Hydrogen (Sc = 0.22), Helium (Sc = 0.30), Oxygen (Sc = 0.60) and Water – vapour (Sc = 0.66) are shown in figure (5). The flow field suffers a decrease in velocity at all points in presence of heavier diffusing species.

The effect of the Hartmann number (M) is shown in figure (6). It is observed that the velocity of the fluid decreases with the increase of the magnetic field number values. The decrease in the velocity as the Hartmann number (M)

increases is because the presence of a magnetic field in an electrically conducting fluid introduces a force called the Lorentz force, which acts against the flow if the magnetic field is applied in the normal direction, as in the present study. This resistive force slows down the fluid velocity component as shown in figure (6). The influence of the viscous dissipation parameter i.e., the Eckert number (Ec) on the velocity and temperature are shown in figures (8) and (12) respectively. The Eckert number (Ec) expresses the relationship between the kinetic energy in the flow and the enthalpy. It embodies the conversion of kinetic energy into internal energy by work done against the viscous fluid stresses. Greater viscous dissipative heat causes a rise in the temperature as well as the velocity. This behavior is evident from figures (8) and (12). The effect of Permeability parameter (K) is presented in the figure (7). From this figure we observe that, the velocity is increases with increasing values of K. The variations of velocity distribution with y for different values of the Dufour number (Du) are shown in figure (10). In this figure, it can be clearly seen that as the Dufour number increases, the velocity increases. The variations of velocity distribution with y for different values of the Soret number (Sr) are shown in figure (9). It can be clearly seen that the velocity distribution in the boundary layer increases with the Soret number. It is interesting note that the effect of Dufour and Soret numbers on velocity field are little significant. This is because either a decrease in concentration difference or an increase in temperature difference leads to an increase in the value of the Soret parameter (Sr). Hence increasing the Soret parameter (Sr) increases the velocity of the fluid.

In figure (11) we depict the effect of Prandtl number $(\Pr)$ on the temperature field. It is observed that an increase in the Prandtl number leads to decrease in the temperature field. Also, temperature field falls more rapidly for water in comparison to air and the temperature curve is exactly linear for mercury, which is more sensible towards change in temperature. From this observation it is conclude that mercury is most effective for maintaining temperature differences and can be used efficiently in the laboratory. Air can replace mercury, the effectiveness of maintaining temperature changes are much less than mercury. However, air can be better and cheap replacement for industrial purpose. This is because, either increase of kinematic viscosity or decrease of thermal conductivity leads to increase in the value of Prandtl number $(\Pr)$. Hence temperature decreases with increasing of Prandtl number $(\Pr)$. Figure (13) depicts the effects of the Dufour number on the fluid temperature. It can be clearly seen from this figure that diffusion thermal effects slightly affect the fluid temperature. As the values of the Dufour number increase, the fluid temperature also increases.

The effects of Schmidt number (Sc) and Soret number (Sr) on the concentration field are presented in figures (14) and (15). Figure (14) shows the concentration field due to variation in Schmidt number (Sc) for the gasses Hydrogen, Helium, Water – vapour, Oxygen and Ammonia. It is observed that concentration field is steadily for Hydrogen and falls rapidly for Oxygen and Ammonia in comparison to Water – vapour. Thus Hydrogen can be used for maintaining effective concentration field and Water – vapour can be used for maintaining normal concentration field. In figure (15), it is observed that an increase in the Soret number (Sr) leads to increase in the concentration field.

The profiles for skin – friction (τ) due to velocity under the effects of Grashof number (Gr), Modified Grashof number (Gc), Prandtl number $(\Pr)$, Schmidt number (Sc), Hartmann number (M), Eckert number (Ec), Soret number (Sr), Dufour number (Du) and Permeability parameter (K) are presented in the table – 1 respectively. We observe from this table – 1, the skin – friction (τ) rises under the effects of Grashof number (Gr), Modified Grashof number (Gc), Eckert number (Ec), Soret number (Sr), Dufour number (Du) and Permeability parameter (K). And falls under the effects of Prandtl number $(\Pr)$, Schmidt number (Sc) and Hartmann number (M).

The profiles for Nusselt number (Nu) due to temperature profile under the effect of Prandtl number $(\Pr)$, Eckert number (Ec) and Dufour number (Du) are presented in the table – 2. From this table we observe that, the Nusselt number (Nu) due to temperature profile rises under the effect of Eckert number (Ec) and Dufour number (Du). And temperature falls under the effect of Prandtl number $(\Pr)$.

Corresponding author: *R. Srinivasa Raju*, Department of Mathematics, Padmasri Dr. B. V. Raju Institute of Technology, Narsapur, Medak, 502313, Andhra Pradesh, India, E-mail: srivass999@gmail.com*

Table – 1: Skin – friction results (τ) for the values of Gr, Gc, Pr, Sc, M, K, Ec, Sr and Du

Gr	Gc	Pr	Sc	M	K	Ec	Sr	Du	τ
1.0	1.0	0.71	0.22	1.0	1.0	0.001	1.0	1.0	3.2954
2.0	1.0	0.71	0.22	1.0	1.0	0.001	1.0	1.0	4.4918
1.0	2.0	0.71	0.22	1.0	1.0	0.001	1.0	1.0	5.3946
1.0	1.0	7.00	0.22	1.0	1.0	0.001	1.0	1.0	2.1650
1.0	1.0	0.71	0.30	1.0	1.0	0.001	1.0	1.0	3.1168
1.0	1.0	0.71	0.22	2.0	1.0	0.001	1.0	1.0	2.6004
1.0	1.0	0.71	0.22	1.0	2.0	0.001	1.0	1.0	3.7905
1.0	1.0	0.71	0.22	1.0	1.0	0.100	1.0	1.0	3.2986
1.0	1.0	0.71	0.22	1.0	1.0	0.001	2.0	1.0	3.3094
1.0	1.0	0.71	0.22	1.0	1.0	0.001	1.0	2.0	3.3118

Table – 2: Rate of heat transfer (Nu) values for different values of Pr, Ec and Du

Pr	Ec	Du	Nu
0.71	0.001	1.0	4.4972
7.00	0.001	1.0	1.0897
0.71	0.100	1.0	4.6270
0.71	0.001	2.0	4.6087

The profiles for Sherwood number (Sh) due to concentration profiles under the effect of Schmidt number (Sc) and Soret number (Sr) are presented in the table – 3. We see from this table the Sherwood number (Sh) due to concentration profile falls under the effect of Schmidt number (Sc) and rises under the effect of Soret number (Sr).

Table – 3: Rate of mass transfer (Sh) values for different values of Sc and Sr

Sc	Sr	Sh
0.22	1.0	6.9193
0.30	1.0	6.5249
0.22	2.0	7.0338

In order to ascertain the accuracy of the numerical results, the present results are compared with the previous results of Ramana Reddy *et al.* [16] for Gr = Gc = 1.0, M = 1.0, Pr = 0.71, and Sc = 0.22 in table – 4. They are found to be in an excellent agreement.

Table – 4: Comparison of present Skin – friction results (τ) with the Skin – friction results (τ^*) obtained by Ramana Reddy *et al.* [16] for different values of Gr, Gc, Sc, Pr and M

Gr	Gc	Pr	Sc	M	τ	τ^*
1.0	1.0	0.71	0.22	1.0	2.5941	2.5705
2.0	1.0	0.71	0.22	1.0	3.0659	2.9984
1.0	2.0	0.71	0.22	1.0	3.6240	3.6191
1.0	1.0	7.00	0.22	1.0	2.1283	2.1150
1.0	1.0	0.71	0.30	1.0	1.9846	1.9716
1.0	1.0	0.71	0.22	2.0	1.5987	1.5889
1.0	1.0	0.71	0.22	1.0	3.0254	3.0018
1.0	1.0	0.71	0.22	1.0	3.1268	3.1047
1.0	1.0	0.71	0.22	1.0	3.2357	3.2286

6. CONCLUSIONS

We summarize below the following results of physical interest on the velocity, temperature and concentration distributions of the flow field and also on the skin – friction, rate of heat and mass transfer at the wall.

1. A growing Hartmann number or Prandtl number or Schmidt number retards the velocity of the flow field at all points.
2. The effect of increasing Grashof number or Modified Grashof number or Permeability parameter or Eckert number or Permeability parameter or Soret number or Dufour number are to accelerate velocity of the flow field at all points.
3. A growing Prandtl number decreases temperature of the flow field at all points and increases with increasing of Eckert number or Dufour number.
4. The Schmidt number decreases the concentration of the flow field at all points and increases with increasing of Soret number.
5. A growing Hartmann number or Prandtl number or Schmidt number decreases the skin – friction while increasing Grashof number or Modified Grashof number or Permeability parameter or Eckert number or Soret number or Dufour number increases the skin – friction.
6. The rate of heat transfer is decreasing with increasing of Prandtl number and increases with increasing of Eckert number and Dufour number.
7. The rate of mass transfer is decreasing with increasing of Schmidt number and increasing with Soret number.
8. On comparing the skin – friction (τ) results with the skin – friction (τ^*) results of Ramana Reddy *et al.* [16] it can be seen that they agree very well.

REFERENCES

[1] Abreu, C. R. A., Alfradique, M. F., and Telles, A. S. Boundary layer flows with Dufour and Soret effects: I: Forced and natural convection, *Chemical Engineering Science*, 61 (2006), 4282 – 4289.
[2] Afify, A. A. Similarity solution in MHD: Effects of thermal diffusion and diffusion thermo on free convective heat and mass transfer over a stretching surface considering suction and injection, *Commun. Nonlinear Sci. Numer Simulat.*, 14 (2009), 2202 – 2214.
[3] Alam, S., Rahman, M. M., Maleque A., and Ferdows, M. Dufour and Soret Effects on Steady MHD Combined Free Forced Convective and mass transfer flow past a Semi Infinite Vertical Plate, *Thammasat Int. J. Sc. Tech.*, 11(2) (2006).
[4] Ambethkar, V. Numerical solutions of heat and mass transfer effects of an unsteady MHD free convective flow past an infinite vertical plate with constant suction. *Journal of Naval Architecture and Marine Engineering*, 5(1) (2008), 27 – 36.
[5] Chin, K. E., Nazar R., Arifin N. M., and Pop, I. Effect of variable viscosity on mixed convection boundary layer flow over a vertical surface embedded in a porous medium. *International Communications in Heat and Mass Transfer*, 34 (2007), 464 – 473.
[6] Gaikwad, S. N., and Malashetty, M. S., and Prasad, K. R. An analytical study of linear and non-linear double diffusive convection with Soret and Dufour effects in couple stress fluid, *International Journal of Nonlinear Mechanics*, 42 (2007), 903 – 913.
[7] Hayat, T., Mustafa, M., and Pop, I. Heat and mass transfer for Soret and Dufour effects on mixed convection boundary layer flow over a stretching vertical surface in a porous medium filled with a viscoelastic fluid. *Communications in Nonlinear Science and Numerical Simulation* 15(5) (2009), 1183 – 1196.
[8] Kafoussias, N. G., and Williams, E. W. Thermal diffusion and diffusion thermo effects on mixed free forced convective and mass transfer boundary layer flow with temperature dependent viscosity, *International Journal of Engineering Science*, 33(9) (1995), 1369 –1384.
[9] Lyubimova, T., Shyklyaeva, E., Legros, J, C., Shevtsova, V. and Roux. Numerical study of high frequency vibration influence on measurement of Soret and diffusion coefficients in low gravity conditions. *Advances in Space Research.* 36 (2005), 70 – 74.
[10] Mansour, M. A., El – Anssary, N. F. and Aly, A. M. Effects of chemical reaction and thermal stratification on MHD free convective heat and mass transfer over a vertical stretching surface embedded in a porous media considering Soret and Dufour numbers, *Journal of Chemical Engineering*, 145(2) (2008), 340 – 345.
[11] Ming – Chun, Li., Yan – wen, T., and Yu – Chun, Z. Soret and Dufour effects in strongly endothermic chemical reaction system of porous media, *Trans. Nonferrous Met. Soc. China*, 16 (2006), 1200 – 1204.
[12] Motsa, S.S. On the onset of convection in a porous layer in the presence of Dufour and Soret effects. *SAMSA Journal of Pure and Applied Mathematics*, 3 (2008),58 – 65.
[13] Mukhopadhyay S. Effect of thermal radiation on unsteady mixed convection flow and heat transfer over a porous stretching surface in porous medium. *International Journal of Heat and Mass Transfer*, 52 (2009), 3261 – 3265.

[14] Osalusi, E., Side. and Harris R. Thermal diffusion and diffusion thermo effects on combined heat and mass transfer of steady MHD convective and slip flow due to a rotating disk with viscous dissipation and Ohmic heating, *International Communications in Heat and Mass Transfer*, 35 (2008), 908 – 915.

[15] Pal, D., and Talukdar, B. Buoyancy and chemical reaction effects on MHD mixed convection heat and mass transfer in a porous medium with thermal radiation and Ohmic heating. *Commun Nonlinear Sci. Numer Simulat.*, 15(10) (2010), 2878 – 2893. DOI: 10.1016/j. cnsns.2009.10.029.

[16] Ramana Reddy, G. V., Ramana Murthy, Ch. V. and Bhaskar Reddy, N. Mixed convective MHD flow and mass transfer past an accelerated infinite vertical porous plate, *Mathematics Applied in Science and Technology*, 1(1) (2009), 65 – 74.

[17] Shateyi, S. Thermal radiation and buoyancy effects on heat and mass transfer over a semi infinite stretching surface with suction and blowing. *Journal of Applied Mathematics, doi:10.1155/2008/414830,* (2008).

[18] Srihari, K., Reddy, S. R., and Rao, J. A. Soret effect on unsteady MHD free convective mass transfer flow past an infinite vertical porous plate with oscillatory suction velocity and heat sink. *International Journal of Applied Mathematical Analysis and Applications* 1(2) (2006), 239 – 259.

[19] Vempati, S. R., and Laxmi – narayana – gari, A. B. Soret and Dufour effects on unsteady MHD flow past an infinite vertical porous plate with thermal radiation. *Appl. Math. Mech. – Engl. Ed.* 31(12) (2010), 1481 – 1496.

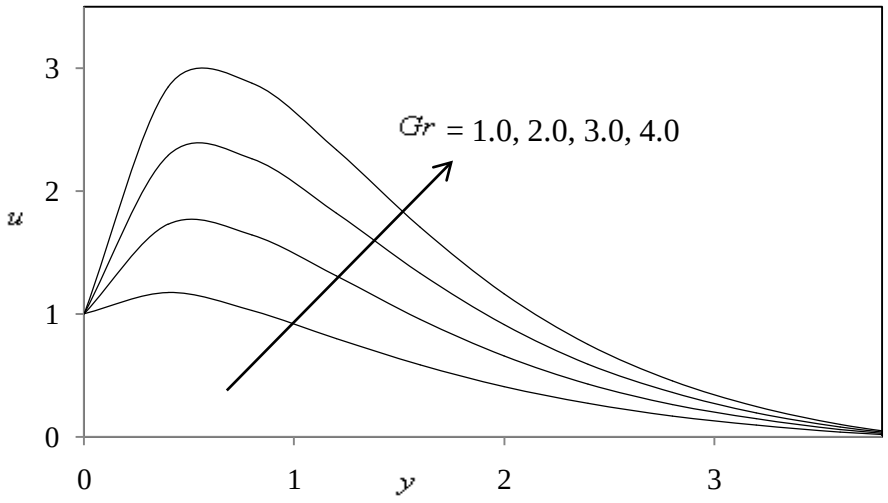

Figure 2. Velocity profiles for different values of Gr

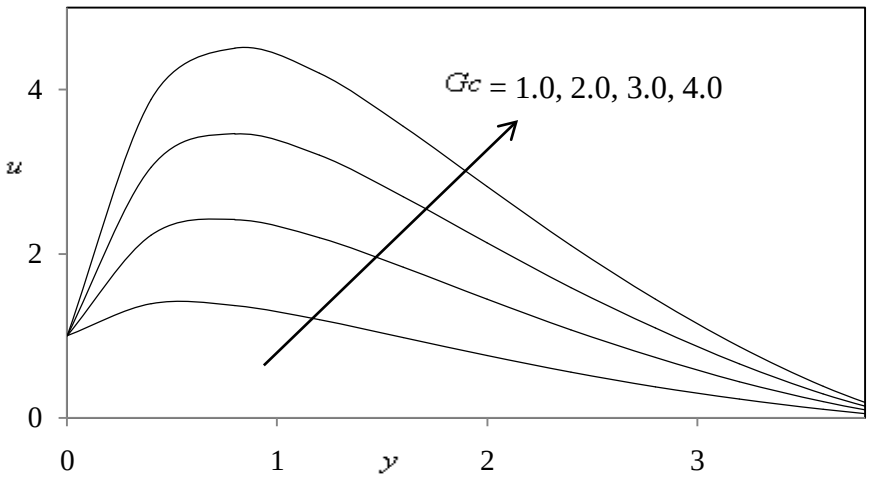

Figure 3. Velocity profiles for different values of Gc

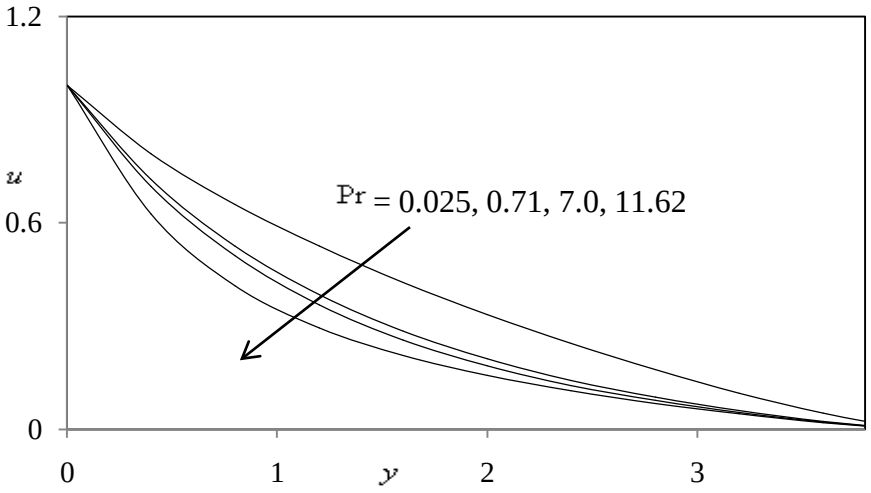

Figure 4. Velocity profiles for different values of Pr

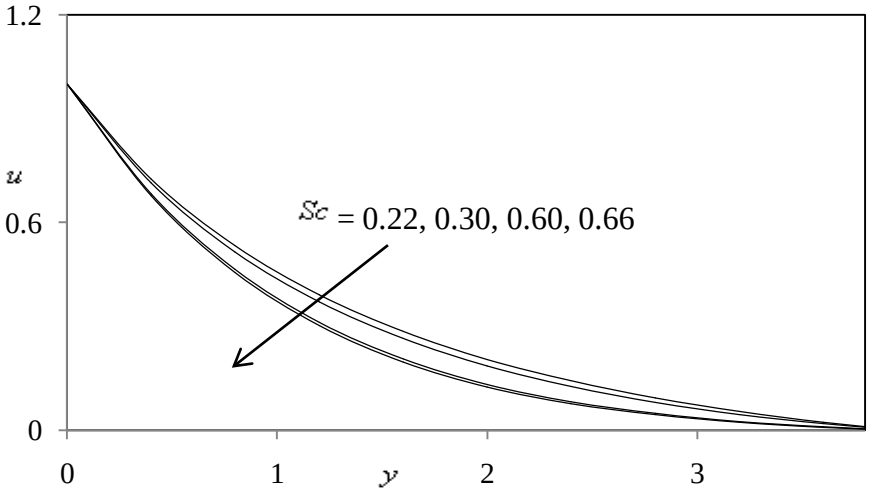

Figure 5. Velocity profiles for different values of Sc

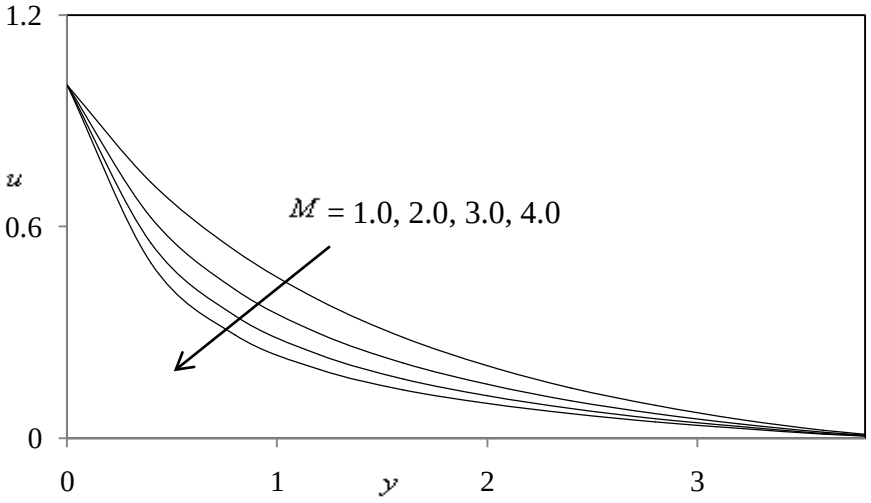

Figure 6. Velocity profiles for different values of M

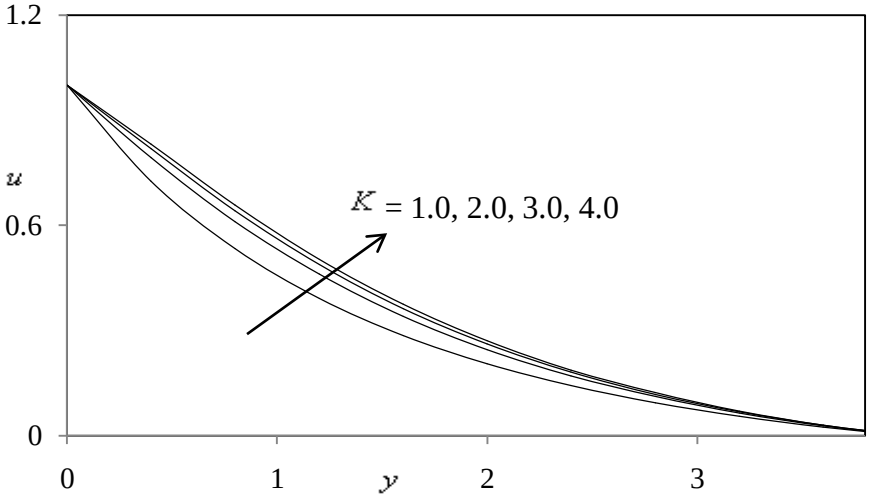

Figure 7. Velocity profiles for different values of K

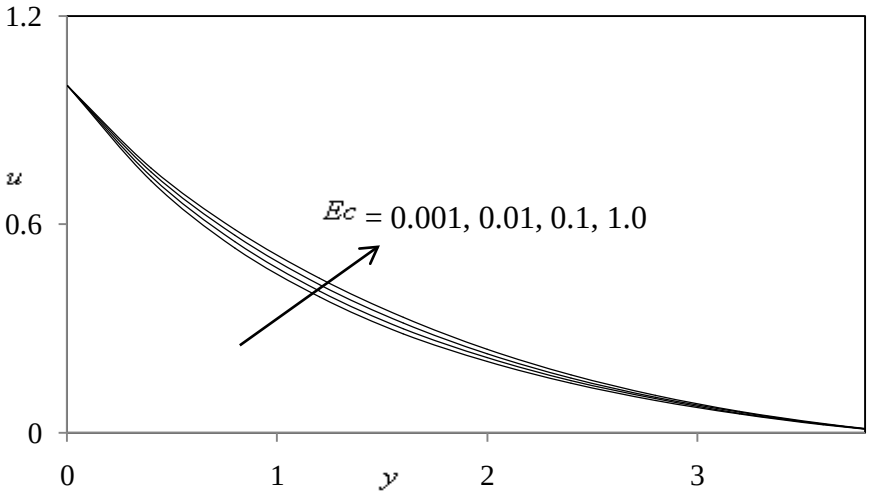

Figure 8. Velocity profiles for different values of Ec

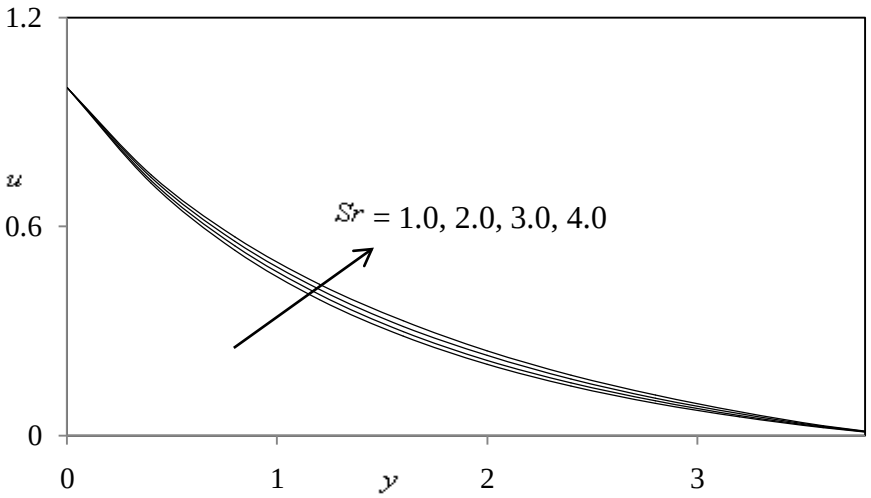

Figure 9. Velocity profiles for different values of Sr

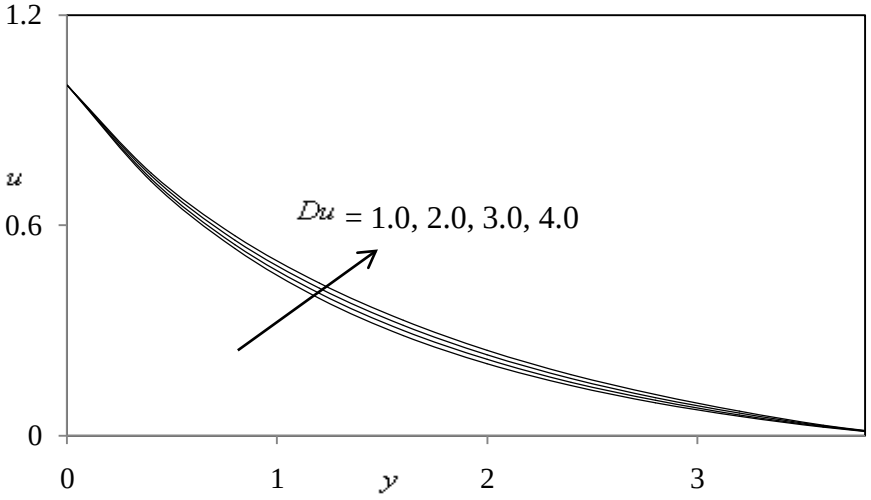

Figure 10. Velocity profiles for different values of Du

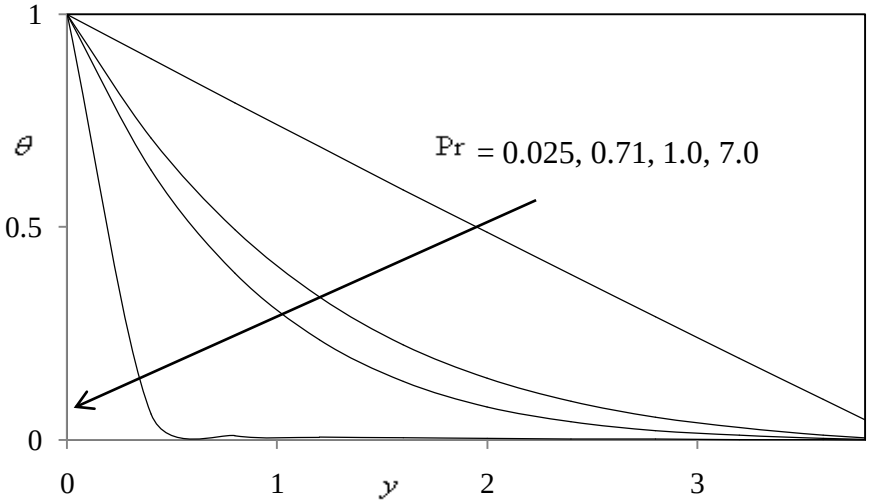

Figure 11. Temperature profiles for different values of Pr

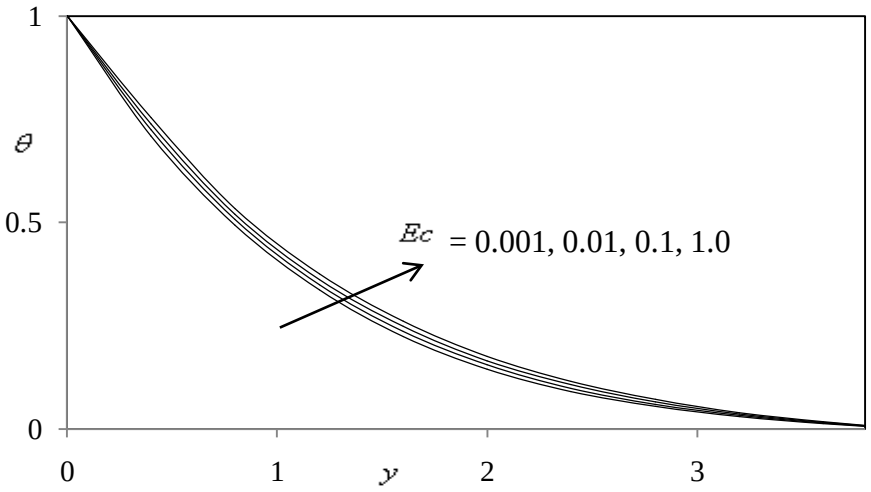

Figure 12. Temperature profiles for different values of Ec

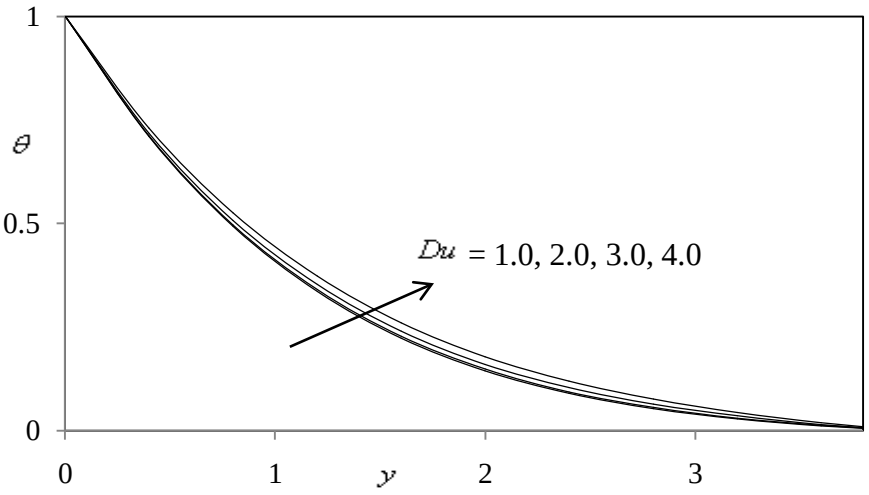

Figure 13. Temperature profiles for different values of Du

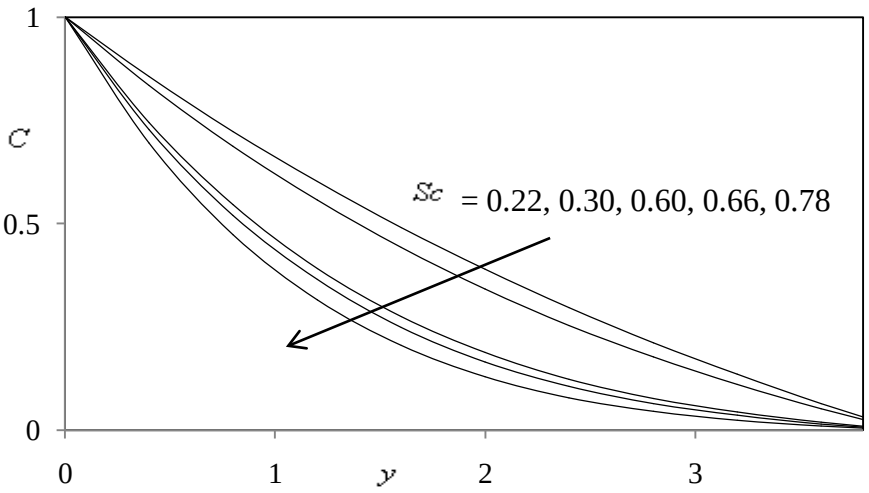

Figure 14. Concentration profiles for different values of Sc

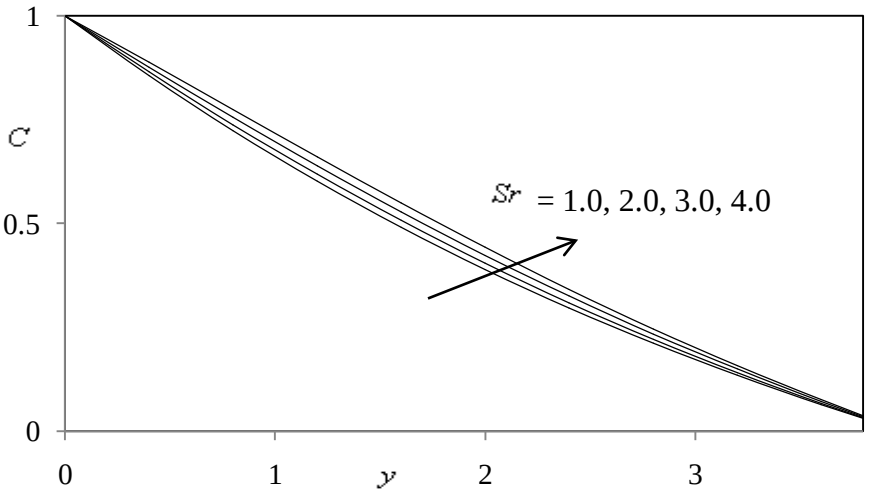

Figure 15. Concentration profiles for different values of Sr

Source of support: Nil, India, Conflict of interest: None Declared

